actuators

MDPI

Article

A Paper-Based Cantilever Beam Mini Actuator Using Hygro-Thermal Response

Laura Alejandra Ireta-Muñoz, Isaias Cueva-Perez, Juan Jose Saucedo-Dorantes and Angel Pérez-Cruz *

Facultad de Ingeniería, Universidad Autónoma de Querétaro, Cerro de las Campanas s/n Querétaro, Querétaro 76000, Mexico; laura.iret@gmail.com (L.A.I.-M.); isaias.cueva@uaq.mx (I.C.-P.); juan.saucedo@uaq.mx (J.J.S.-D.)

* Correspondence: angel.perez@uaq.mx

Abstract: New technological and scientific advances in the development of sensors and actuators demand the development of new devices to deal with recent problems and challenges in these new and emerging processes. Moreover, paper-based devices have tremendous potential for developing actuators as paper exhibits capillary transport and hygroexpansion due to swelling of the fibers when absorbing water. Therefore, this paper proposes a mini actuator that is based on a hygro-thermal-paper-based cantilever beam that is activated by means of a droplet of an aqueous solution in combination with a circulating electrical current to analyze its response. The contribution of this proposal includes the analysis of the flexural response of the mini actuator when it is tested by using two different solutions: distilled water and a water/alcohol solution. Additionally, four cases related to the droplet volume are studied and a statistical analysis of the bending responses is presented. The results achieved show that that water-alcohol solutions have a lower deviation in comparison with water only. Moreover, it is demonstrated that a specific change in the maximum displacement is obtained according to the volume and the type of solution. Thus, it is suggested that the response of the mini actuator can be tuned using different aqueous solutions.

Keywords: mini actuator; paper-based sensor; hygroexpansion

Citation: Ireta-Muñoz, L.A.; Cueva-Perez, I.; Saucedo-Dorantes, J.J.; Pérez-Cruz, A. A Paper-Based Cantilever Beam Mini Actuator Using Hygro-Thermal Response. *Actuators* **2022**, *11*, 94. https://doi.org/10.3390/act11030094

Academic Editor: Jose Luis Sanchez-Rojas

Received: 28 January 2022
Accepted: 9 March 2022
Published: 17 March 2022

1. Introduction

Currently, new technological and scientific advances are leading to complex processes in different fields; additionally, emerging technology has led to new challenges that must be addressed. On the other side, the increasing demands of large deformation devices such as wearable sensors have also led to the use of different materials in which flexibility and softness properties have been of interest. Additionally, the flexibility of soft materials has been exploited, aiming to implemented and/or apply and evaluate it in soft pneumatic actuators (SPAs) fabricated with an injection of air and silicone rubber coating [1]. Accordingly, magnetic actuators have also been implemented with soft materials to control locomotion in robots [2–4]. In this regard, the electromechanical response of soft materials has been evaluated using polymer composites to associate the actuator displacement with the changes in dielectric constant [5]. Particularly, thermal actuators have been implemented using the bending response caused by the application of an electric field which is related to the speed of actuator response, aiming to provide solutions for recent applications [6]. However, challenges have recently arisen in the development of new actuators; the fabrication process requires a long time or specialized equipment to fabricate such devices. Moreover, the material is non-biodegradable. For this reason, the investigation of biodegradable materials has gained importance in the development of actuators [7]. On the other hand, paper and graphene have been used and combined to contribute to the development of strain sensors [8]. In this sense, the flexibility of these materials has been also exploited for the development of soft-actuators and humidity sensors [9]. Likewise, other properties such as electrical resistance have been also analyzed in order to provide feasible routes for constructing efficient sensors that may produce efficient electrical stimuli [10]. Yet although recent studies have contributed and lead to significative advances, a drawback has arisen, as this material requires specialized treatment for its deposition on paper.

Paper-based microfluidic systems have been broadly studied due to the characteristics associated with the acronym ASSURED (Affordable, Sensitive, Specific, User-Friendly, Rapid and Robust, Equipment Free, Deliverable to all end-users) [11]. These characteristics have been exploited and have led to the development of diverse systems such as lab-on-a-chip devices in applications such as the photoelectrochemical (PEC) visual sensing systems [12,13]; additionally, they have been implemented in analytical devices that represent affordable solutions, capable of measuring microfluidic responses [14,15], and such characteristics have intentionally led to the design and development of sophisticated devices that have been implemented as a part of personalized health care procedures including emergency, ambulatory, and remote areas [16]. Additionally, it should be highlighted that properties such as biodegradability and low cost make paper a suitable option for the development of gas, humidity, strain, and pressure sensors [17–19]. Other application fields are involved with the development of sensors in medical applications, such as using paper for physiological monitoring [20], where properties such as the elasticity of paper have been the object of study for the design and fabrication of wearable devices [21]. Furthermore, the flexibility of paper has also been considered for the implementation of wearable devices in health monitoring [22,23].

Therefore, the aforementioned properties, such as biodegradability and flexibility, have been studied to evaluate the response of paper to different actuation stimuli [24]. One of the most important properties is its mechanical response which has been studied and addressed through the analysis of the response under tension and compression loads [25]. These properties have been implemented together with the electric response of the material to develop electromechanical actuators [26]. Electroactive paper (EAPap), which bends when an electric field is applied to the electrodes of the device [27], has actuation principles that have been implemented using different combinations of materials [28]. Thermal actuation has also been used to measure bending angles in a bonding beam made of graphite paper and polyimide film (PI) when an electric field is applied [29]. Furthermore, the response to temperature gradients has also been implemented for the design of electric switches [30]. The motion in paper-based systems has been also studied under the effects of fluid-related phenomena such as capillarity [31] and moisture gradients that cause curling on paper [32]. Relative and local humidity changes have also been associated with the mechanical response of paper bending by hygroexpansion [33] and have been combined with the use of light irradiation [34]. Hamedi et al. at [35] implemented a hygroexpansive electrothermal paper actuator (HEPA) in a bilayer configuration which consists of paper, conducting polymer, and adhesive tape. This device uses a conductive path to generate the necessary heat, and in combination with the principle of absorption of moisture causes actuation. Moreover, the influence of humidity and temperature changes on the mechanical response of paper-based actuators has been studied using numeric methods [36]. These humidity-based actuators have a faster response to humidity changes and a good response to the thermal effect generated by the conductive path, but the control of humidity was implemented in a controlled chamber with a humidifier. Nevertheless, the use of a localized moisture gradient caused by a droplet has not been implemented to induce actuator movement. This actuation principle may be of interest in the field as it can be fully integrated with paper-based microfluidic devices.

Therefore, this paper proposes a hygro-thermal-mechanical paper-based mini actuator triggered by a microliter droplet of an aqueous solution. The mini actuator consists of a cantilever beam with a conductive path to accelerate the evaporation time of aqueous solutions. To evaluate the flexural actuator response, different solution volumes were tested in the actuator. The local increment of moisture content on the mini actuator is produced by a droplet of an aqueous solution placed directly on the surface of the mini actuator with a micropipette. The movement is induced by the hygroexpansion effect, and the 'going-back' motion through the evaporation which is accelerated by a current across the conductive path. Two aqueous solutions were used to evaluate the response of the actuator: distilled water, used as a reference case, and a mix of distilled water with alcohol using different volumes. It was found that the maximum deflection produced by the actuation principle is associated with the solution volume and that the time response to reverse this motion is associated with the solution's characteristics. The results show that distilled water with alcohol produces a faster actuation in comparison with distilled water due to the faster evaporation of alcohol.

2. Materials and Methods

In this section the working principle, materials, and experimental set up are described. Likewise, the proposed mini actuator and tuning response by droplet volumes are presented.

2.1. Mini Actuator Working Principle

The matrix of cellulose-based materials provides an excellent medium to transport liquids without external forces. When paper interacts with liquids, its mechanical properties are modified, i.e., by the softening of paper and the reduction in its elasticity module [37–39]. This is caused by the interaction between the liquid and the cellulose fibers. The cellulose fibers are expanded or contracted due to this interaction. As a result, deformation phenomena such as creeping, waving, curling, and deflection are observed at the macroscopic level [40]. Perez et al. [41] took advantage of this phenomenon by developing a paper-based device for the characterization of binary aqueous solutions. This was achieved by modelling the bending response of a paper-based cantilever beam. However, this response is in the static/quasi-static domain due to the slowness of the deflection response. The increasing demand of eco-friendly, affordable, and portable devices involving paper-based mechanical systems demands more knowledge about the dynamic behavior of humidified/wetted paper to produce paper-based actuators with faster responses.

The proposed mini actuator is based on the hygro-thermal-mechanical response of paper that consists of a cantilever beam with a conductive path that was fabricated to accelerate the evaporation time of the aqueous solutions. Its working principle is depicted following its activation response, which is induced by means of the imbibition of an aqueous solution into the cantilever beam paper. The activation is illustrated precisely in Figure 1. First, Figure 1a shows the proposed mini actuator in its initial position, where the left end is the fixed end, which is connected to a current supply. Afterwards, a droplet of an aqueous solution is deposited onto the surface of the cantilever beam, as can be seen in Figure 1b; subsequently, the fibers of paper swell as their moisture content increases—this is namely hygroexpansive strain. It has been suggested that swelling takes place as the water molecules break and replace interchain bonds in cellulose [41]. As an example, Figure 2 shows the hygroexpansive strain of dry and wet chromatography paper. In this case, the hygroexpansive strain of 0.17 is measured along the thickness of the paper. Thus, the motion or the activation response is produced due to the differential expansion of paper and the conductive layer; this is represented in Figure 1c. As the thermal linear expansion of the silver conductive path is in the order of 10^{-3} while the hygroexpansion is two orders of magnitude greater (10^{-1}), the contribution of thermal expansion is neglected in this work. Finally, aiming to reduce the deactivation time (deswelling of fibers) of the actuator due to drying process of paper, the heating produced by the conductive electrode incorporated on the top of the beam leads the actuator to return to its initial position once is fully dried, as depicted in Figure 1d. The conductive path has been designed to reach a maximum temperature of approximately 40 °C to not compromise the integrity of paper but provide heating to dry the mini actuator once is wetted after activation, following Ansari and Cho [42].

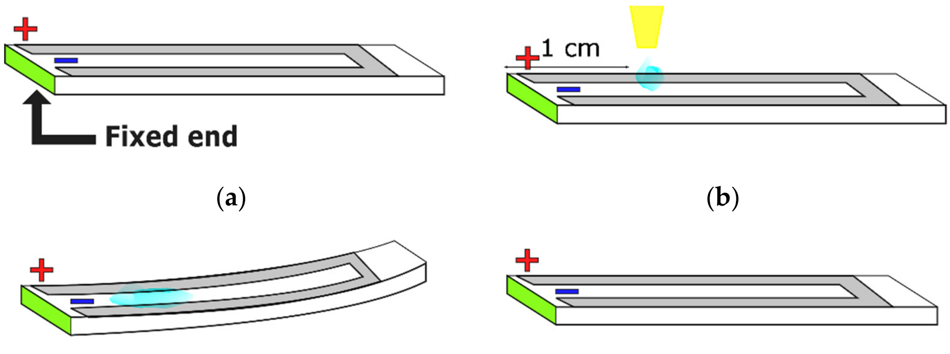

Figure 1. Schematic of the actuation principle: (**a**) Initial position; (**b**) Activation by volume solution; (**c**) Movement induced by hygroexpansion; (**d**) Deactivation/deswelling induced by current heating; return to initial position.

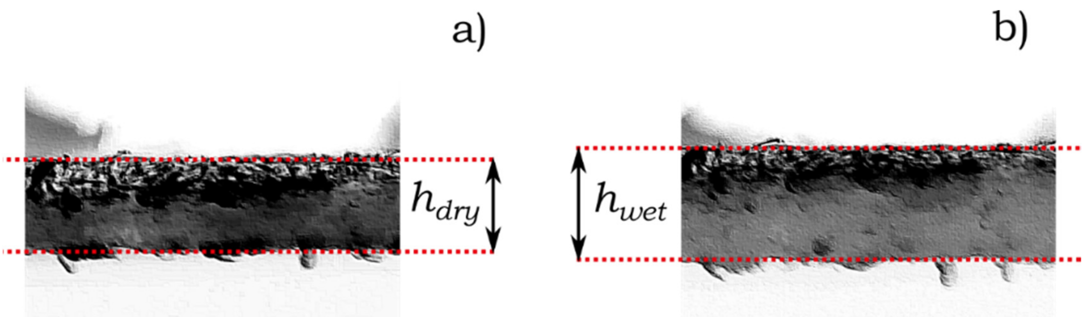

Figure 2. Microscope cross section image of a piece of chromatography paper experiencing hygroexpansive strain along its thickness. Comparison of (**a**) dry thickness (hdry) and (**b**) wet thickness (hwet).

The reaction produced in the cantilever beam is quantified measuring the displacement at the free end of the actuator; the whole activation procedure is shown in Figure 3. In this sense, the mini actuator has an initial position as described in Figure 3a; this initial position belongs to pinpoint (a) in the graph at initial time. Subsequently, the mini actuator remains connected to the control current for five minutes. After this period, a droplet solution is added to the beam as shown in Figure 3b; afterward, the paper hygroexpansion induces a movement until a maximum displacement is reached; this located in the graph as pinpoint (c) and is depicted by Figure 3c. Finally, due to the temperature reached due to the conductive path, the actuator tip returns to a point that is close to its initial position.

2.2. Experimental Set Up

To evaluate the performance of the proposed paper-based mini actuator, different cantilever beams were designed with similar geometrical characteristics such as a length, width, and thickness of 35 mm, 5 mm, and 1 mm, respectively. All the actuators are made of filter CST paper from Triton Electronics Ltd., Dunmow, Essex, UK. The silver conductive ink is hand-printed on top of the cantilever beam; silver was selected because of its good performance on porous materials like paper and because it remains over the top layer and is not imbibed into the paper fibers. The shape and dimensions of the conductive path are selected to ensure a specific resistance value of 2.9 ohms. Thus, the geometrical representation of the proposed paper-based mini actuator, as well as the materials employed, are presented in Figure 4a; it can be observed that the conductive path is located on top of the filter paper and has a width of 1 mm. The beams are cut out manually using a conventional knife, trying to retain as much similarity as possible. Thus, the final size of the cantilever beam may be compared to the real size of a two-euro coin, which is portrayed in Figure 4b.

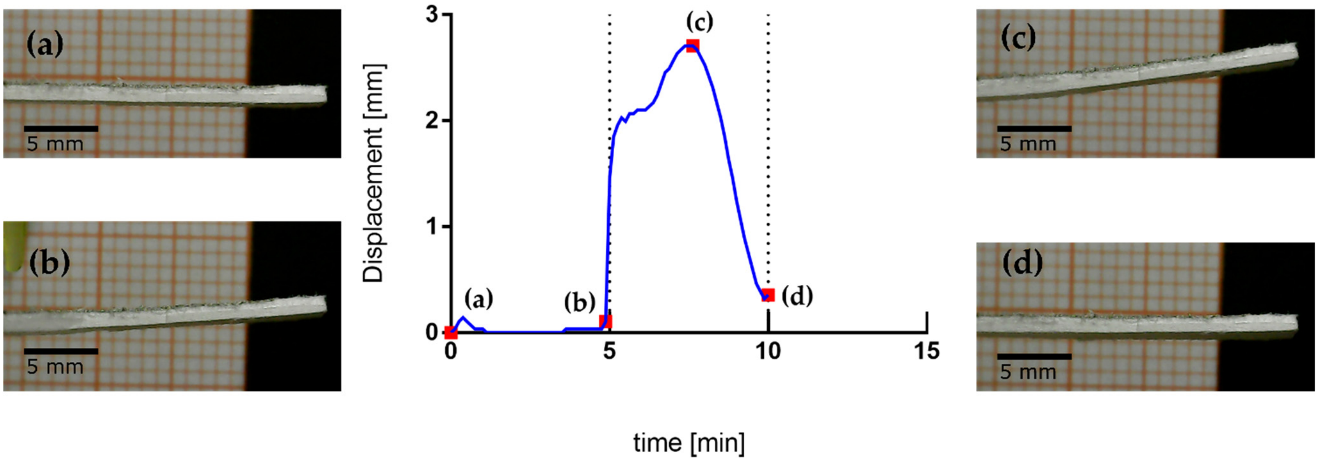

Figure 3. Activation/deactivation of paper cantilever-beam: (**a**) Initial position when connected to current control; (**b**) After 5 min, activation by volume solution; (**c**) Maximum displacement induced by hygroexpansion; (**d**) Deactivation/evaporation induced by current; return to initial position.

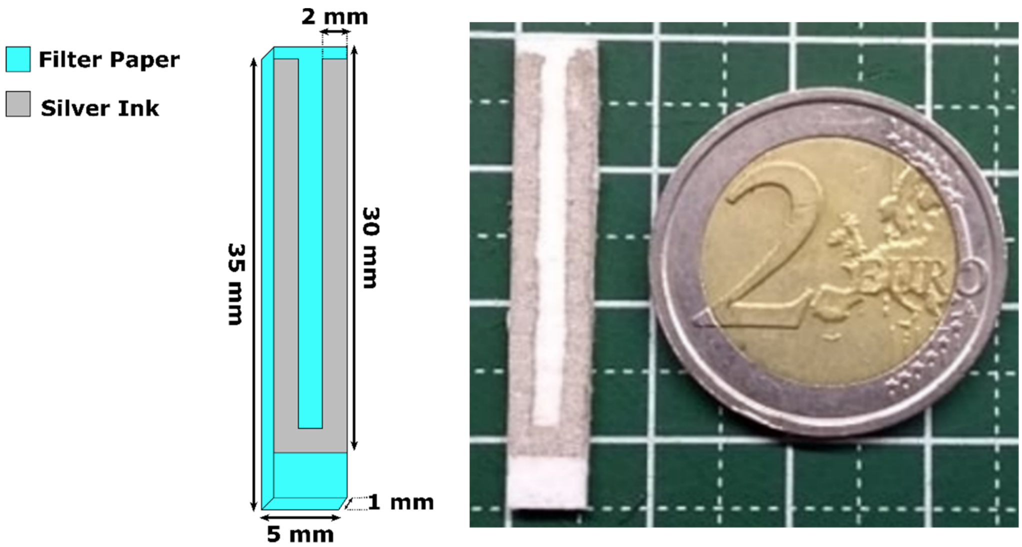

Figure 4. Comparative geometry schematic for sample mini actuator (**a**) Geometry and materials of mini actuator; (**b**) Representation of the silver conductive ink hand printed on top of the cantilever beam and its size compared with a two euro coin.

The experiment was performed in a controlled environment under laboratory conditions; in Figure 5, the complete experimental test bench is shown, and consists of a box of Plexiglas, with a holder to fix one of the ends of the cantilever beam (Figure 5A). In order to ensure the repeatability of the experiments, the experimental test bench also includes a support for the pipette and an illumination system in order to take pictures for post-processing purposes (Figure 5B). To capture and measure the deflection response of the cantilever beam, several pictures were acquired by handheld microscope and stored in a personal computer (Figure 5C). Each tested beam was electrically connected to current control circuitry to heat the conductive path during the experiment (Figure 5D). For further details on control circuity please refer to Supplementary Figure S1. As can be observed in Figure 5D, the current control was connected to a mini actuator using a connector. Finally, the circuitry was connected to a regulated power supply designed to deliver 5V and to feed the illumination system (Figure 5E).

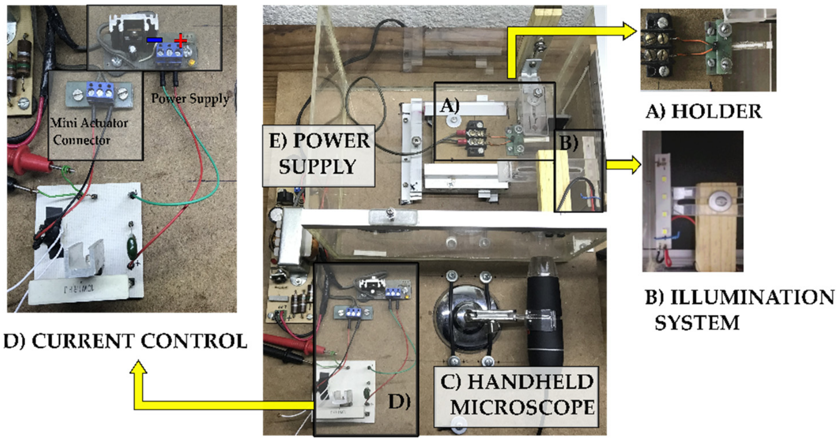

Figure 5. Experimental setup used for testing and to validate the proposed mini actuator composed by: (**A**) the holder, (**B**) the illumination system, (**C**) the handheld microscope, (**D**) the current control, and (**E**) the power supply.

2.3. Tuning Response of the Mini Actuator

Aiming to tune the response of the actuator produced by a distilled water droplet (20 µL), the actuator response was first evaluated without the application of current. The obtained response can be observed in Figure 6, where the red curve represents the actuator response without current application; as can be observed, the actuator produced a flexural response where the bending activation was faster than deactivation. Such a phenomenon is due to the deactivation procedure taking a long time, since there is no current flow in the conductor path and the temperature of the actuator cannot be increased; consequently, the paper fibers take a long time to dry out. On the other side, also in Figure 6, the blue curve depicts the obtained response related to the flexural displacement when several drops of water are deposited in the actuator and when its conductive path is connected to current control for adding heat. Due to the actuator path being subjected to current excitation, an increase in the actuator temperature is achieved, allowing a faster dry-out; as can be observed in Figure 6, the return to the initial position becomes faster with each droplet of solution deposited. The current values are measured when the actuator path is subjected to the current flow; thus, Figure 7 shows the current values measured during the experiment each activation. It is possible to observe that variation in current values remains in a range of 385 to 458 mA, which ensures the maximum temperature calculated.

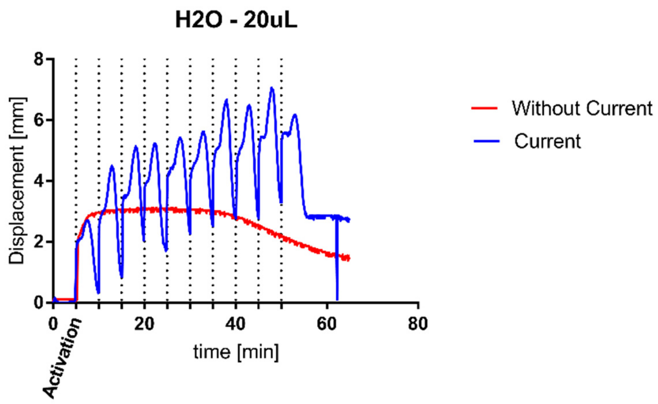

Figure 6. Activation/deactivation time of paper-beam for 20 µL distilled water.

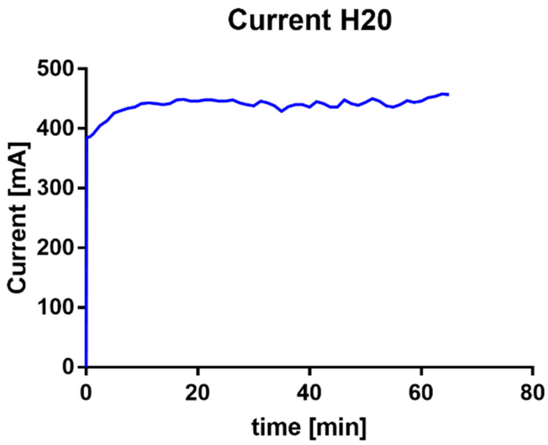

Figure 7. Current measured during experiment with 20 µL of aqueous solution.

Although the conductive path is set to reach a maximum of 40 °C, it is expected that the wetting activation of the paper-based actuator has a key role on the thermal response of the beam. In this case, the authors proposed two means of tuning the response of the mini actuator: (i) controlling the amount of heat while using water, and (ii) using alternative aqueous solutions while setting a constant current throughout the conductive path. The latter is adopted in this work; thus, a binary solution of distilled water and alcohol is suggested for tuning the mini actuator response as its evaporation rate is faster than that of distilled water. Moreover, a tuning of the bending response of the mini actuator by varying the volume of water-alcohol is proposed. It is expected that, with a decrease in the volume of solution deposited, the amplitude of deflection would decrease, for two reasons. First, as the volume of liquid is decreased, a small hygroexpansion would occur. Second, with a low volume of droplets deposited on the beam, the time for drying would be reduced.

In this regard, the displacement measurement was performed for seven samples per volume deposited, which consisted of 20 µL of distilled water, and 20 µL, 15 µL, and 10 µL of distilled water with alcohol in a proportion 50/50 *v/v*. The proposed volume of the solution was selected by trial and error with the purpose of assessing the actuator response. Due to its evaporation rate, the actuator response should return to the initial position faster than in the distilled water case. The droplet was placed between the larger edges of the beam, at 1 cm of length measured from the fixed end of the sample, as was shown previously in Figure 2b. Subsequently, this experiment consisted of supplying a current level to the mini actuator for 65 min to obtain ten activations per each tested cantilever beam. The movement activation in the beam was performed by adding a droplet of solution to the sample every 5 min; this time was selected because it was observed that it represents the mean time that a sample requires to return to the reference point. Subsequently, pictures of the beam were handled by a microscope, which was configured with a sampling time of 7.4 s; the pictures were processed with the software ImageJ to obtain the displacement change in the sample. In Figure 8a, a representation of the reference point for an initial time is shown. Figure 8b illustrates the maximum deflection at the free end of the beam and the reference level (dashed yellow line).

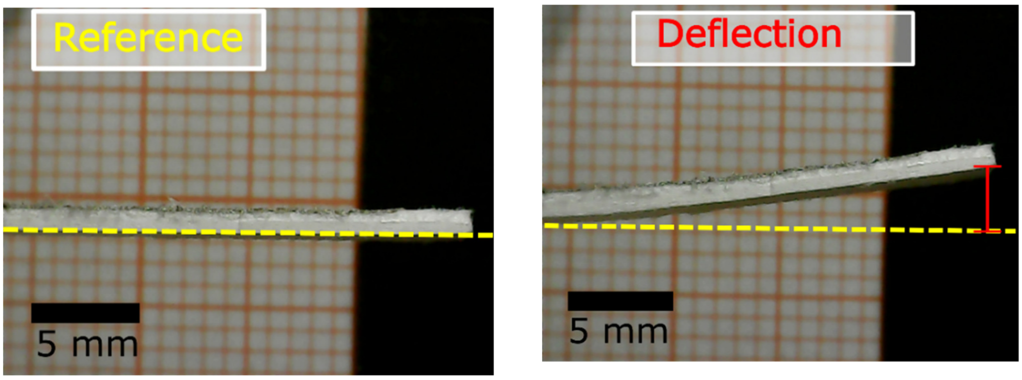

(**a**) (**b**)

Figure 8. Deflection measurement of the free end of the sample to measure the displacement changes with respect to the reference line: (**a**) Reference guideline; (**b**) Measure deflection.

3. Results and Discussions

The results achieved support and validate the proposed mini actuator and are presented in this section as well as the details and discussion regarding each experiment performed. In order to obtain statistically significant results, a set of ten activations in a row were performed on each mini actuator to evaluate its performance. Thus, in Figure 9 the displacements per beam for each corresponding amount of solution are represented graphically. As can be observed, the achieved displacements are reported in millimeters; in particular, the first case corresponds to a solution of 20 µL of distilled water [H_2O] as is shown in Figure 9a. Hence, Figure 9a shows the behavior of the seven beams and the activation obtained by the addition of a micro droplet of water every five minutes. Moreover, as can be observed, the measured displacement presents an increase that is associated with the activation of each droplet solution by the addition of a micro droplet of water every five minutes. During the experimentation, it was noticed that for some cases the displacement of the beam rarely returned to the reference point. This phenomenon was present because the water was absorbed by cellulose fibers due to hygroexpansion. For that reason, the response obtained and shown in Figure 9a presents the curve tendency for each sample displacement increased with time without reaching the reference point.

Accordingly, the remained of the experiments were carried out using a binary solution composed of distilled water-alcohol. The alcohol used in this experiment was ethanol, which produces a faster drying process in the paper due to its higher volatility, in comparison with the volatility of water. It is well known that volatility depends on the strength of the liquid intermolecular bonds; in this regard, water has stronger intermolecular bonds in comparison with ethanol. Therefore, it is easier for ethanol to break the interface between liquid and gas when kinetic energy is added to the liquid. In this case, the kinetic energy is added through the Joule effect caused by the current circulating in the conductive path. Thus, it can be concluded that solutions in which water is mixed with ethanol have a faster drying process. In this way, the second case also considers a solution volume of 20 µL of distilled water-alcohol; the solution was applied as previously described in Figure 9b, where the achieved increases in displacement are shown. As can be appreciated, the resulting tendency shows behavior that is contrary to the first case of study (Figure 9a); specifically, the reference point is reached by each activation. This is because the evaporation time is faster due to the chemical properties of alcohol. Likewise, Figure 9c,d show the obtained displacements that belong to the third and fourth cases of study, that is, for 15 µL and 10 µL, respectively. As can be observed in Figure 9c,d, the maximum displacement reached by each activation is smaller than in the two previous cases. Additionally, the same behavior is observed in the third and fourth cases of study. Through these obtained results, it can be concluded that the maximum displacement is associated with fiber expansion due to the solution volume.

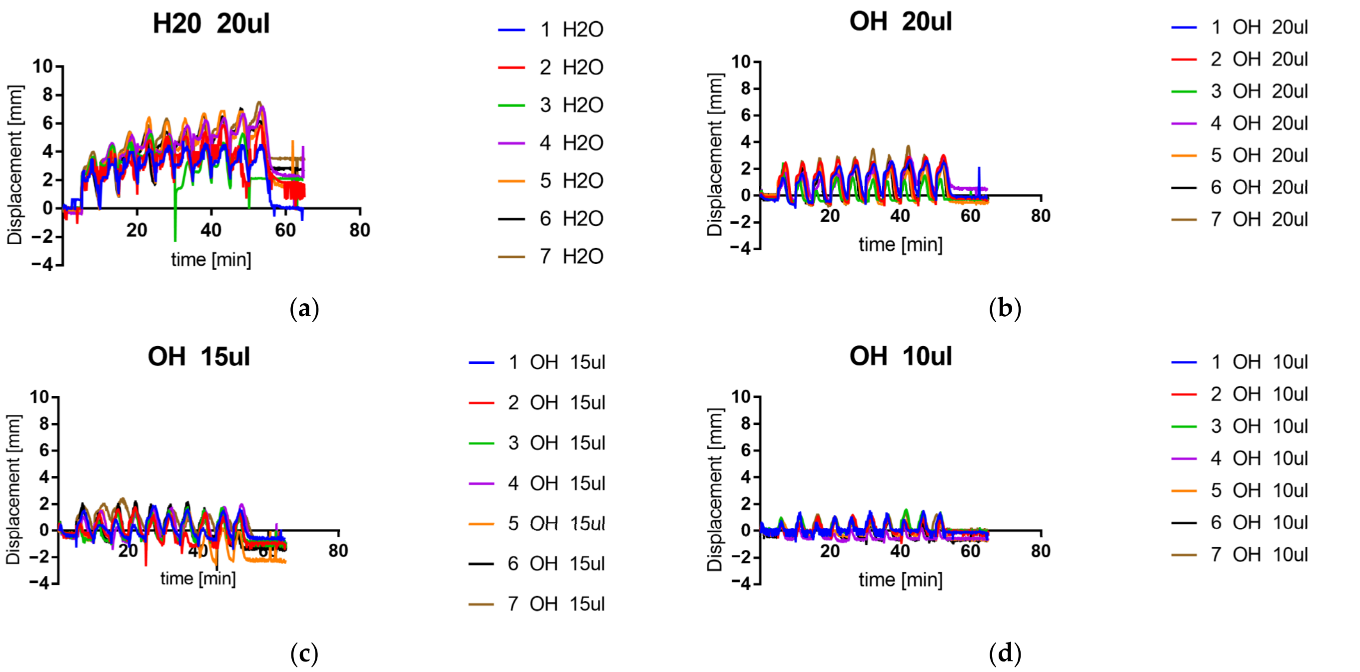

Figure 9. Measured displacement of each sample per amount of solution: (**a**) 20 µL distilled water; (**b**) 20 µL distilled water with alcohol (OH); (**c**) 15 µL distilled water with alcohol (OH); (**d**) 10 µL distilled water with alcohol (OH).

Furthermore, the experimental results show that the displacement per sample is different for each type and volume solution. For this reason, in order to complement the achieved results, a statistical analysis was performed by estimating the maximum and mean/average displacement. Thus, the average displacement and the maximum displacement were first computed for each analyzed sample; afterwards, the average values per each case of study were obtained for both the mean displacement and the maximum displacement, averaging the results obtained for each sample. Such comparison was performed among the studied samples, estimating the standard deviation. As a result, the maximum displacement average and the standard deviation for each experiment are shown in Figure 10, where the horizontal axis corresponds to each study case and the vertical axis represents the mean value. The error bar corresponds to one standard deviation. Specifically, in Figure 10a the results obtained for maximum displacement are shown; here, a tendency for the displacement to increase is observed. The values reached for the binary solutions were 1.144 mm, 1.917 mm, and 2.827 mm for the cases of 10 µL, 15 µL, and 20 µL, respectively. On the other side, for the test with 20 µL of distilled water a maximum average value of 6.340 mm was obtained, which is the highest value of all the cases evaluated. Here, it can be noted that the use of a binary solution not only reduces the time response but also the hygroexpansion of paper. The error bar for the case of water is greater than the other cases; this may be related to the evaporation rate and the large deformations of the beam due to the high expansion of the fibers. In Figure 10b the mean values for each case of study are shown; as can be observed, the tendency is not clear due to the quantity of values computed and slight differences between each case.

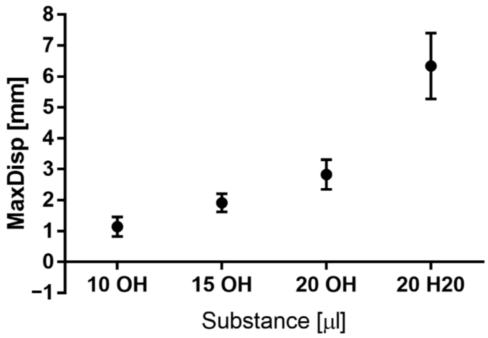

(a)

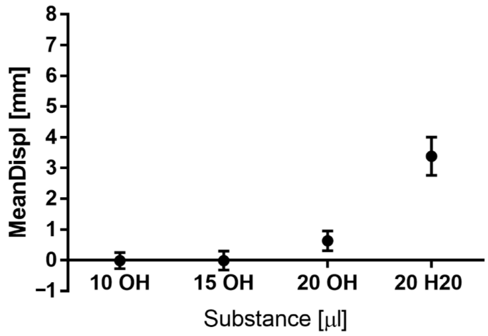

(b)

Figure 10. Mean values per study case: (**a**) Maximum displacement; (**b**) Mean displacement.

4. Conclusions

In this work, a hygro-thermal-mechanical paper-based mini actuator triggered by a microliter droplet of an aqueous solution was proposed. The novelty of this proposal considers the design of the mini actuator to be installed as a cantilever beam with a conductive path that leads to accelerated evaporation times of the aqueous solutions. The proposed mini actuator is validated by its evaluation through its flexural response with different solution volumes. In this regard, the response of the mini actuator was evaluated for four cases. The first case study was carried out with distilled water, using 20 µL of solution. The following three cases corresponded to the binary solution of alcohol and distilled water. The amount of liquid placed on the samples in each experiment was 10, 15, and 20 µL. From the results of these studies, it was concluded that the maximum displacement measured for each case was associated with the amount and type of solution. Thus, it is possible to tune the response of the mini actuators using other aqueous solutions. Additionally, the results suggest that the proposed mini actuator is suitable for microfluidic applications, as it is activated by liquid transport, and its application in different fields may lead to the solution of recent challenges/drawbacks that cannot be addressed by conventional actuators. An automated calibration procedure based on embedded circuit technology could be developed in future works, as well as numerical modeling of the thermal and wetting phenomena to improve the design and to ensure the repeatability of the device, with regard to the displacement levels that were reached in this present work. Furthermore, the development of the proposed mini actuator should lead to new devices that can be used in several applications in the field of microfluidics—certainly, in applications such as electrochemical biosensors and piezoelectric biosensors.

Supplementary Materials: The following supporting information can be downloaded at: https://www.mdpi.com/article/10.3390/act11030094/s1, Figure S1: Current Control Diagram.

Author Contributions: Conceptualization, A.P.-C. and L.A.I.-M.; methodology, A.P.-C. and J.J.S.-D.; validation, I.C.-P. and L.A.I.-M.; formal analysis, I.C.-P. and L.A.I.-M.; writing—original draft preparation, L.A.I.-M. and I.C.-P.; writing—review and editing, A.P.-C. and J.J.S.-D. All authors have read and agreed to the published version of the manuscript.

Funding: This research was partially supported by the National Council on Science and Technology of Mexico (CONACYT) through the scholarship 312230.

Informed Consent Statement: Not applicable.

Data Availability Statement: Data available on request.

Acknowledgments: The authors acknowledge the technical support for the experimental set up provided by Fernando Ireta Moreno.

Conflicts of Interest: The authors declare no conflict of interest.

References

1. Oguntosin, V.; Abdulkareem, A. Design of a pneumatic soft actuator controlled via eye tracking and detection. *Heliyon* **2020**, *6*, e04388. [CrossRef]
2. Venkiteswaran, V.K.; Tan, D.K.; Misra, S. Tandem actuation of legged locomotion and grasping manipulation in soft robots using magnetic fields. *Extreme Mech. Lett.* **2020**, *41*, 101023. [CrossRef]
3. Tang, D.; Zhang, C.; Sun, H.; Dai, H.; Xie, J.; Fu, J.; Zhao, P. Origami-inspired magnetic-driven soft actuators with programmable designs and multiple applications. *Nano Energy* **2021**, *89*, 106424. [CrossRef]
4. Fu, C.; Xia, Z.; Hurren, C.; Nilghaz, A.; Wang, X. Textiles in soft robots: Current progress and future trends. *Biosens. Bioelectron.* **2022**, *196*, 113690. [CrossRef]
5. Kirkman, S.; Rothemund, P.; Acome, E.; Keplinger, C. Electromechanics of planar HASEL actuators. *Extreme Mech. Lett.* **2021**, *48*, 101408. [CrossRef]
6. Zhao, G.; Yang, J.; Wang, Y.; Zhao, H.; Wang, Z. Preparation and electromechanical properties of the chitosan gel polymer actuator based on heat treating. *Sens. Actuators A Phys.* **2018**, *279*, 481–492. [CrossRef]
7. Migliorini, L.; Santaniello, T.; Rondinini, S.; Saettone, P.; Comes Franchini, M.; Lenardi, C.; Milani, P. Bioplastic electromechanical actuators based on biodegradable poly(3-hydroxybutyrate) and cluster-assembled gold electrodes. *Sens. Actuators B Chem.* **2019**, *286*, 230–236. [CrossRef]
8. Qi, X.; Li, X.; Jo, H.; Sideeq Bhat, K.; Kim, S.; An, J.; Kang, J.; Lim, S. Mulberry paper-based graphene strain sensor for wearable electronics with high mechanical strength. *Sens. Actuators Phys.* **2020**, *301*, 111697. [CrossRef]
9. Jia, G.; Zheng, A.; Wang, X.; Zhang, L.; Li, L.; Li, C.; Zhang, Y.; Cao, L. Flexible, biocompatible and highly conductive MXene-graphene oxide film for smart actuator and humidity sensor. *Sens. Actuators B Chem.* **2021**, *346*, 130507. [CrossRef]
10. Wang, W.; Liu, D.; Liu, Y.; Leng, J.; Bhattacharyya, D. Electrical actuation properties of reduced graphene oxide paper/epoxy-based shape memory composites. *Compos. Sci. Technol.* **2015**, *106*, 20–24. [CrossRef]
11. Smith, S.; Korvink, J.G.; Mager, D.; Land, K. The potential of paper-based diagnostics to meet the ASSURED criteria. *RSC Adv.* **2018**, *8*, 34012–34034. [CrossRef]
12. Zhang, L.; Kong, Q.; Li, L.; Wang, Y.; Ge, S.; Yu, J. Direct-readout photoelectrochemical lab-on-paper biosensing platform based on coupled electricity generating system and paper supercapacitors. *Talanta* **2021**, *222*, 121517. [CrossRef] [PubMed]
13. Kong, Q.; Cui, K.; Zhang, L.; Wang, Y.; Sun, J.; Ge, S.; Zhang, Y.; Yu, J. "on-Off-On" Photoelectrochemical/Visual Lab-on-Paper Sensing via Signal Amplification of CdS Quantum Dots@Leaf-Shape ZnO and Quenching of Au-Modified Prism-Anchored Octahedral CeO_2 Nanoparticles. *Anal. Chem.* **2018**, *90*, 11297–11304. [CrossRef] [PubMed]
14. Ozer, T.; McMahon, C.; Henry, C.S. Advances in Paper-Based Analytical Devices. *Annu. Rev. Anal. Chem.* **2020**, *13*, 85–109. [CrossRef] [PubMed]
15. Lim, W.Y.; Goh, B.T.; Khor, S.M. Microfluidic paper-based analytical devices for potential use in quantitative and direct detection of disease biomarkers in clinical analysis. *J. Chromatogr. B Analyt. Technol. Biomed. Life. Sci.* **2017**, *1060*, 424–442. [CrossRef] [PubMed]
16. Mahato, K.; Srivastava, A.; Chandra, P. Paper based diagnostics for personalized health care: Emerging technologies and commercial aspects. *Biosens. Bioelectron.* **2017**, *96*, 246–259. [CrossRef] [PubMed]
17. Tai, H.; Duan, Z.; Wang, Y.; Wang, S.; Jiang, Y. Paper-Based Sensors for Gas, Humidity, and Strain Detections: A Review. *ACS Appl. Mater. Interfaces* **2020**, *12*, 31037–31053. [CrossRef] [PubMed]
18. Long, Y.; He, P.; Xu, R.; Hayasaka, T.; Shao, Z.; Zhong, J.; Lin, L. Molybdenum-carbide-graphene composites for paper-based strain and acoustic pressure sensors. *Carbon* **2020**, *157*, 594–601. [CrossRef]
19. Lee, D.; Kim, D. Paper-Based, Hand-Painted Strain Sensor Based on ITO Nanoparticle Channels for Human Motion Monitoring. *IEEE Access* **2019**, *7*, 77200–77207. [CrossRef]
20. Huang, Y.; Wang, Z.; Zhou, H.; Guo, X.; Zhang, Y.; Wang, Y.; Liu, P.; Liu, C.; Ma, Y.; Zhang, Y. Highly sensitive pressure sensor based on structurally modified tissue paper for human physiological activity monitoring. *J. Appl. Polym. Sci.* **2020**, *137*, 48973. [CrossRef]
21. Liu, H.; Qing, H.; Li, Z.; Han, Y.L.; Lin, M.; Yang, H.; Li, A.; Lu, T.J.; Li, F.; Xu, F. Paper: A promising material for human-friendly functional wearable electronics. *Mater. Sci. Eng. R Rep.* **2017**, *112*, 1–22. [CrossRef]
22. Liu, Y.; Wang, H.; Zhao, W.; Zhang, M.; Qin, H.; Xie, Y. Flexible, Stretchable Sensors for Wearable Health Monitoring: Sensing Mechanisms, Materials, Fabrication Strategies and Features. *Sensors* **2018**, *18*, 645. [CrossRef] [PubMed]
23. Wang, X.; Liu, Z.; Zhang, T. Flexible Sensing Electronics for Wearable/Attachable Health Monitoring. *Small* **2017**, *13*, 1602790. [CrossRef] [PubMed]
24. Liu, Y.; Shang, S.; Mo, S.; Wang, P.; Yin, B.; Wei, J. Soft actuators built from cellulose paper: A review on actuation, material, fabrication, and applications. *J. Sci. Adv. Mater. Devices* **2021**, *6*, 321–337. [CrossRef]
25. Li, Y.; Stapleton, S.E.; Reese, S.; Simon, J.W. Anisotropic elastic-plastic deformation of paper: Out-of-plane model. *Int. J. Solids Struct.* **2018**, *130–131*, 172–182. [CrossRef]
26. Kanaparthi, S.; Sekhar, V.R.; Badhulika, S. Flexible, eco-friendly and highly sensitive paper antenna based electromechanical sensor for wireless human motion detection and structural health monitoring. *Extreme Mech. Lett.* **2016**, *9*, 324–330. [CrossRef]
27. Kim, J. Chapter 7—Nanocellulose-based paper actuators. In *Nanocellulose Based Composites for Electronics*; Thomas, S., Pottathara, Y.B., Eds.; Elsevier: Amsterdam, The Netherlands, 2021; pp. 163–183. [CrossRef]

28. Khan, A.; Abas, Z.; Kim, H.; Kim, J. Recent Progress on Cellulose-Based Electro-Active Paper, Its Hybrid Nanocomposites and Applications. *Sensors* **2016**, *16*, 1172. [CrossRef] [PubMed]
29. Fan, Q.; Miao, J.; Tian, M.; Zhao, H.; Zhu, S.; Liu, X.; Ma, Y.; Qu, L. Low-voltage Driven Flexible Double-layer Electrothermal Actuator for Smart Human-machine Interactions. *Sens. Actuators Phys.* **2020**, *315*, 112352. [CrossRef]
30. Shin, S.; So, H. Time-dependent motion of 3D-printed soft thermal actuators for switch application in electric circuits. *Addit. Manuf.* **2021**, *39*, 101893. [CrossRef]
31. Ha, J.; Kim, H.Y. Capillarity in Soft Porous Solids. *Annu. Rev. Fluid Mech.* **2020**, *52*, 263–284. [CrossRef]
32. Brandberg, A.; Motamedian, H.R.; Kulachenko, A.; Hirn, U. The role of the fiber and the bond in the hygroexpansion and curl of thin freely dried paper sheets. *Int. J. Solids Struct.* **2020**, *193–194*, 302–313. [CrossRef]
33. Kumar, A.; Heidari-Bafroui, H.; Charbaji, A.; Rahmani, N.; Anagnostopoulos, C.; Faghri, M. Numerical and Experimental Modeling of Paper-Based Actuators. *Chem. Proc.* **2021**, *5*, 15. [CrossRef]
34. Weng, M.; Tang, Z.; Zhu, J. Multi-responsive soft paper-based actuators with programmable shape-deformations. *Sens. Actuators Phys.* **2021**, *331*, 113016. [CrossRef]
35. Hamedi, M.M.; Campbell, V.E.; Rothemund, P.; Güder, F.; Christodouleas, D.C.; Bloch, J.; Whitesides, G.M. Electrically Activated Paper Actuators. *Adv. Funct. Mater.* **2016**, *26*, 2446–2453. [CrossRef]
36. Zhou, L.; Nie, B.; Ren, S.; Żur, K.K.; Kim, J. On the hygro-thermo-electro-mechanical coupling effect on static and dynamic responses of piezoelectric beams. *Compos. Struct.* **2021**, *259*, 113248. [CrossRef]
37. Lee, M.; Kim, S.; Kim, H.Y.; Mahadevan, L. Bending and buckling of wet paper. *Phys. Fluids* **2016**, *28*, 042101. [CrossRef]
38. Douezan, S.; Wyart, M.; Brochard-Wyart, F.; Cuvelier, D. Curling instability induced by swelling. *Soft Matter.* **2011**, *7*, 1506–1511. [CrossRef]
39. Reyssat, E.; Mahadevan, L. How wet paper curls. *Europhys. Lett.* **2011**, *93*, 54001. [CrossRef]
40. Cueva-Perez, I.; Perez-Cruz, A.; Stiharu, I.; Dominguez-Gonzalez, A.; Trejo-Hernandez, M.; Osornio-Rios, R.A. A parametric study on the nonlinear dynamic response of paper-based mechanical systems due to liquid transport. *Int. J. Non-Linear Mech.* **2020**, *118*, 103280. [CrossRef]
41. Perez-Cruz, A.; Stiharu, I.; Dominguez-Gonzalez, A. Nonlinear imbibition influence on the hygro-mechanical bending response of paper due to its interaction with water. *Int. J. Non-Linear Mech.* **2017**, *97*, 89–95. [CrossRef]
42. Ansari, M.Z.; Cho, C. A conduction–convection model for self-heating in piezoresistive microcantilever biosensors. *Sens. Actuators A Phys.* **2012**, *175*, 19–27. [CrossRef]